

Electronic Supplementary Information

Role of Urea on Structural, Textural, and Optical Properties of Macroemulsion-assisted Synthesized Holey ZnO Nanosheets for Photocatalytic Applications

Amelia Andriani,^a Didi Prasetyo Benu,^{a,b,c} Vetty Megantari,^a Brian Yuliarto,^{d,e} Rino Rakhmata Mukti,^{a,e,f} Yusuke Ide,^g Silvia Chowdhury,^h Mohammed A. Amin,ⁱ Yusuf Valentino Kaneti,^{h*} and Veinardi Suendo^{a,e*}

^a *Division of Inorganic and Physical Chemistry, Faculty of Mathematics and Natural Sciences, Institut Teknologi Bandung, 10 Ganesha Street, Bandung 40132, Indonesia.*

^b *Doctoral Program of Chemistry Faculty of Mathematics and Natural Sciences, Institut Teknologi Bandung, 10 Ganesha Street, Bandung 40132, Indonesia.*

^c *Department of Chemistry, Universitas Timor, Kefamenanu 85613, Indonesia.*

^d *Advanced Functional Materials (AFM) Laboratory, Engineering Physics Department, Institut Teknologi Bandung, 10 Ganesha Street, Bandung 40132, Indonesia.*

^e *Research Center for Nanosciences and Nanotechnology, Institut Teknologi Bandung, 10 Ganesha Street, Bandung 40132, Indonesia.*

^f *Center for Catalysis and Reaction Engineering, Institut Teknologi Bandung, 10 Ganesha Street, Bandung 40132, Indonesia.*

^g *International Center for Materials Nanoarchitectonics (WPI-MANA), National Institute for Materials Science (NIMS), 1-1 Tsukuba, Ibaraki 305-0044, Japan.*

^h *Australian Institute for Bioengineering and Nanotechnology (AIBN), The University of Queensland, Brisbane, QLD 4072, Australia.*

ⁱ *Department of Chemistry, College of Science, Taif University, P. O. Box 11099, Taif 21194, Saudi Arabia.*

E-mails: y.kaneti@uq.edu.au (Y. V. Kaneti); v.suendo@chem.itb.ac.id (V. Suendo)

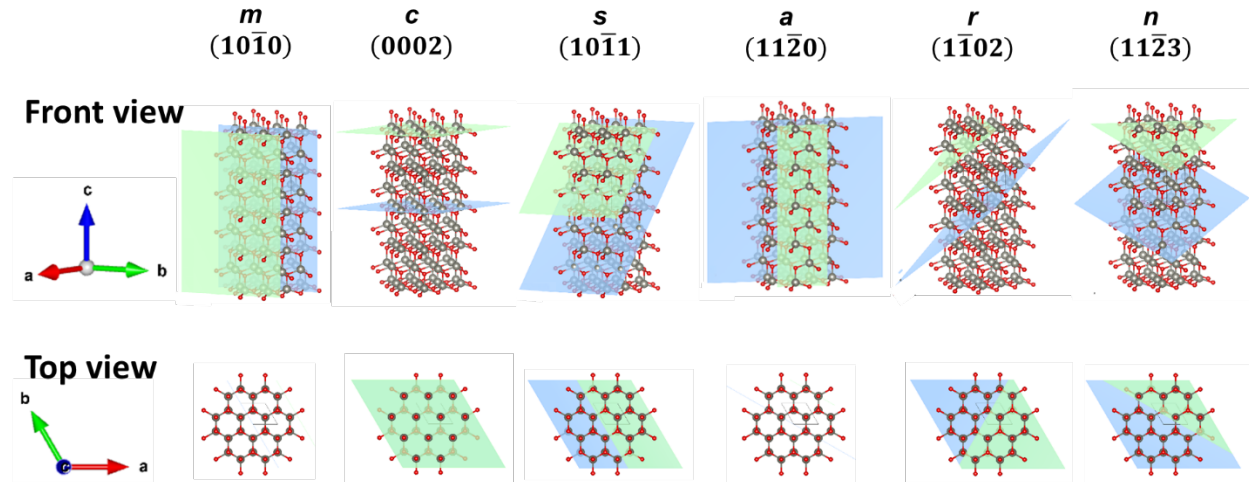


Fig. S1. Front view and top view of the six different low-index crystallographic planes in wurtzite ZnO (CIF 2300450, Crystallography Open Database), red and grey atoms represent O and Zn, respectively.

Table S1. Recent studies on the morphology-controlled syntheses of zinc oxide and their properties.

Synthesis method	Morphology	BET surface area ($\text{m}^2 \text{ g}^{-1}$)	Average pore diameter (nm)	Total pore volume ($\text{cm}^3 \text{ g}^{-1}$)	Bandgap energy	Ref.
Homogeneous precipitation	Hierarchically structured aggregates	84.0	16.0	0.253	N/A	1
Interface precipitation	Hierarchically structured aggregates	60.0	27.0	0.242		
Microwave hydrothermal and solvothermal process	Marigold-flower like	16.6	22.0	0.05	3.194	2
	Multipod-jasmine-flower like	14.7	19.5	0.07	3.157	
	Sea urchin-rod-flower like	12.6	38.7	0.11	3.153	
	Calendula-flower like	10.7	11.3	0.02	3.147	
	Rice-grain-shape like	14.9	18.4	0.16	3.114	

Synthesis method	Morphology	BET surface area ($\text{m}^2 \text{ g}^{-1}$)	Average pore diameter (nm)	Total pore volume ($\text{cm}^3 \text{ g}^{-1}$)	Bandgap energy	Ref.
Solvothermal process	Prism	15.5	N/A	N/A	N/A	3
	Polyhedron	20.1				
	Sphere	12.9				
Hydrothermal process	Hexagonal microstructure	4.30	N/A	N/A	2.99	4
		8.40			3.11	
		27.6			3.11	
		32.0			3.11	
	Doughnuts like	94.7			3.11	
Schlenk techniques	Nanocones	12.1	N/A	N/A	3.21	5
	Nanorods	15.6			3.15	
Microwave processing of a precipitate	Cone-shaped	19.1	14.2	0.0710	3.36	6
	Thin platelike aggregates	24.8	20.5	0.1147	3.35	
	Cone-shaped	15.5	25.7	0.0732	3.36	
Refluxed process	Nanosheets	83.0	7-16	N/A	3.21	7
	Nanorods	18.0	N/A	N/A	3.18	
	Nanodisks	46.0	5-8	N/A	3.15	
Thermal decomposition	Nanopyramids	N/A	N/A	N/A	3.20	8
Hydrothermal process	Nanoflakes				3.27	
	Nanocolumns				3.24	
Hydrothermal process	Hexagonal column	N/A	N/A	N/A	3.15-3.20	9
	Double hexagonal column				3.13-3.21	
Microemulsion method	Hexagonal-disk	35.0	N/A	N/A	3.35	10
	Brick-type	25.0			3.33	
	Sharp needle-like	23.0			3.31	
Microwave process	Nanospheroidal	N/A	N/A	N/A	3.20-3.24	11
Low-temperature hydrothermal processing of a precipitate	Micro-rods	N/A	N/A	N/A	3.16	12
	Partly ordered hexagonal prism rods				3.17	
	Ordered hexagonal prism rods				3.18	
	Ellipsoids				3.19	
	Spheroids				3.20	
	Nanospheres				3.22	

Synthesis method	Morphology	BET surface area ($\text{m}^2 \text{ g}^{-1}$)	Average pore diameter (nm)	Total pore volume ($\text{cm}^3 \text{ g}^{-1}$)	Bandgap energy	Ref.
Simple wet chemical method	Nanoflower	N/A	N/A	N/A	3.40	¹³
Sol-gel chemical process	Hexagonal rods	N/A	N/A	N/A	3.20	¹⁴
	A mix of thin hexagonal rods and wide slates				3.22	
	Globular shaped particle-like structure				3.33	
	Very short hexagonal rods				3.19	
Solvothermal process	Hexagonal nanoplates	14.4	N/A	N/A	N/A	¹⁵
	Nanorods	7.43				
Hydrothermal process	Nanoflakes	20.9	N/A	N/A	N/A	¹⁶
Refluxed process	Nanosheets	25.7	N/A	N/A	N/A	¹⁷
Thermal decomposition	Flower-like nanorods	N/A	N/A	N/A	3.37	¹⁸
Solvothermal process	Hexagonal tetrakaidecahedral	17.7	N/A	N/A	N/A	¹⁹
	Pencil stub-like	4.76				
Hydrothermal process	Flower-like aggregates	21.8	3.8	0.042	N/A	²⁰

Table S2. Detailed amounts of all chemicals used to synthesize the ZnO products reported in this study.

Sample name	Composition					
	Zn(CH ₃ COO) ₂ ·2H ₂ O (g)	Urea (g)	CTAB (g)	H ₂ O (mL)	Toluene (mL)	Butanol (mL)
ZnO_U0	1.4553	0	0.4957	11.87	17.17	1.21
ZnO_U0.5	1.4457	0.1966	0.4925	11.80	17.06	1.20
ZnO_U1	1.4363	0.3907	0.4893	11.72	16.95	1.19
ZnO_U2	1.4179	0.7713	0.4830	11.57	16.73	1.18

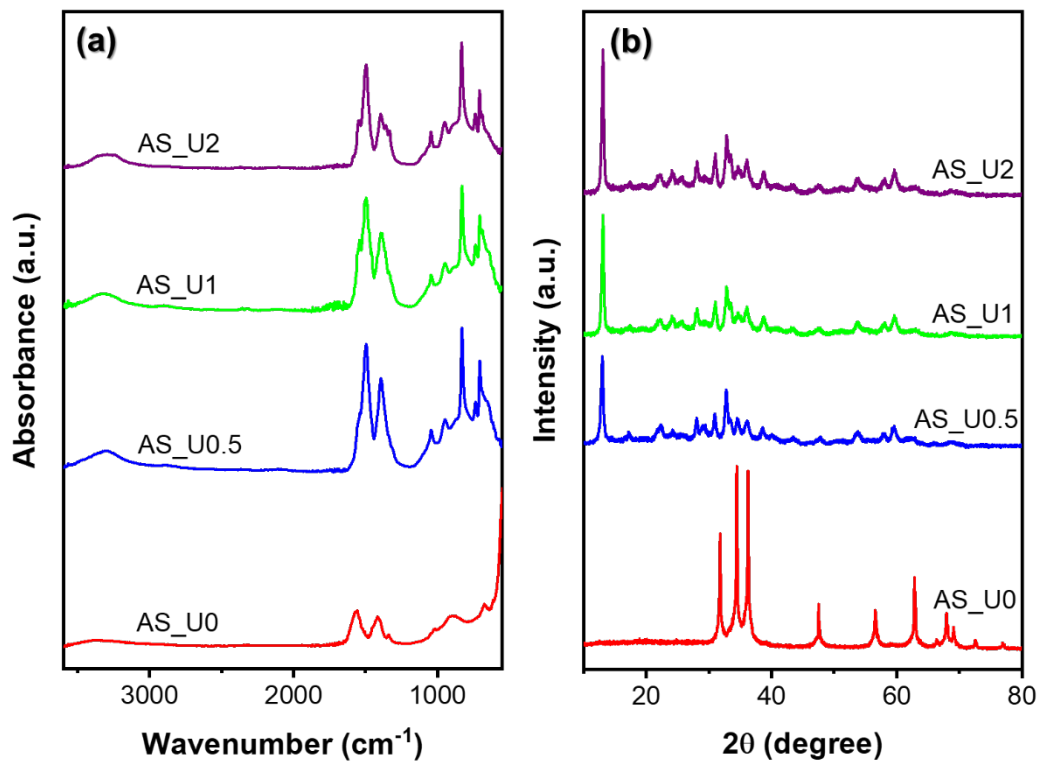


Fig. S2. Structural analyses of as-synthesized products before calcination: (a) FTIR spectra and (b) XRD patterns.

Table S3. Rietveld refinement parameters of synthesized ZnO samples

Sample name	R_p (%)	R_{wp} (%)	R_{exp} (%)	χ^2
ZnO_U0	12.2	15.0	12.4	1.466
ZnO_U0.5	13.1	16.1	15.9	1.030
ZnO_U1	13.2	16.0	15.7	1.039
ZnO_U2	10.0	13.2	12.6	1.860

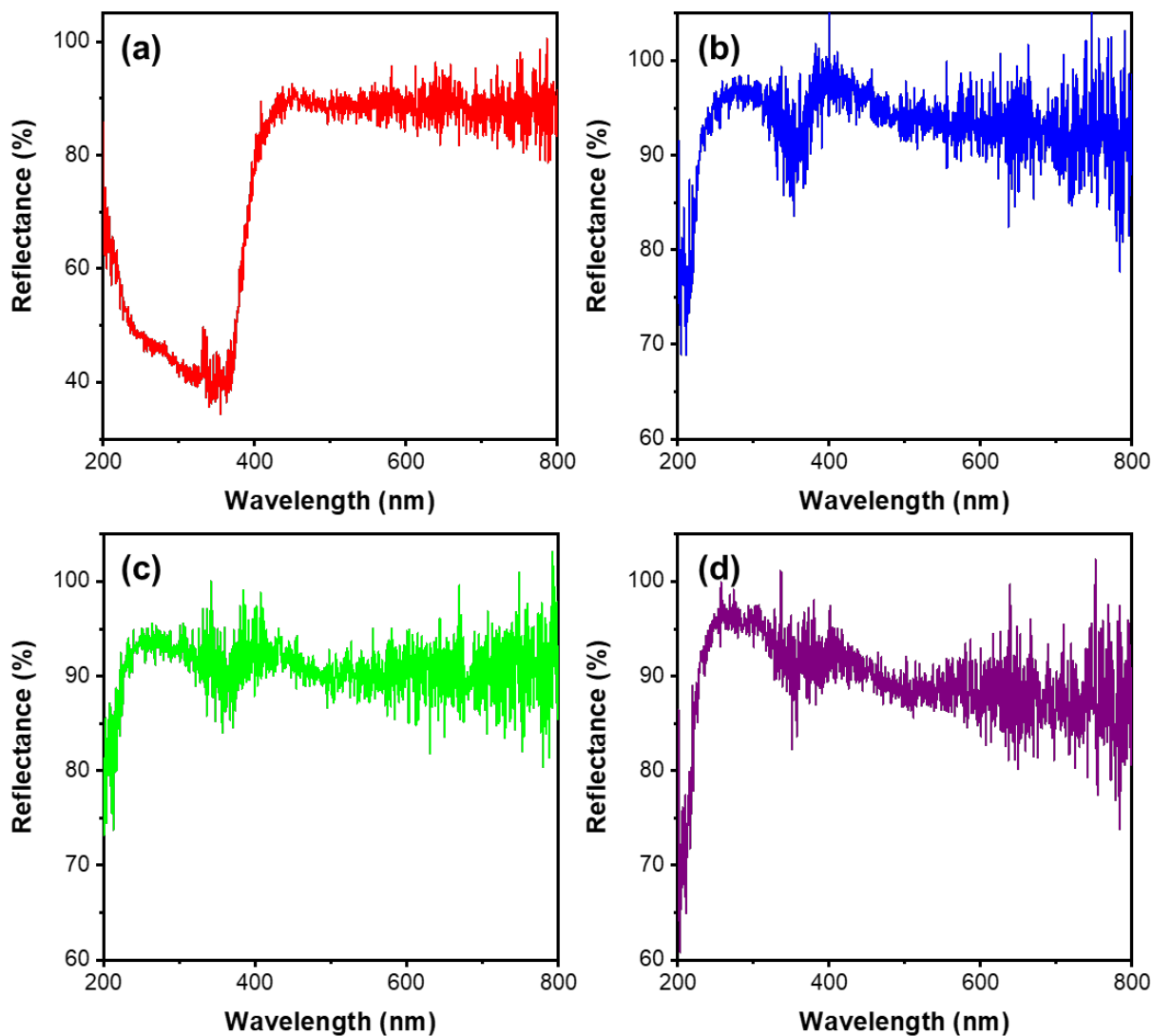


Fig. S3. UV-vis diffuse reflectance spectra of as-synthesized samples before calcination: (a) AS_U0, (b) AS_U0.5, (c) AS_U1, and (d) AS_U2.

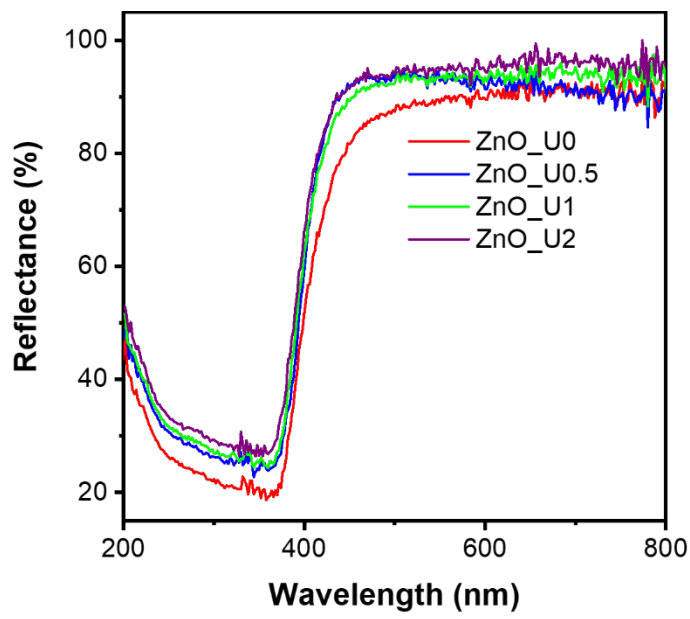


Fig. S4. UV-vis diffuse reflectance spectra of the synthesized ZnO samples.

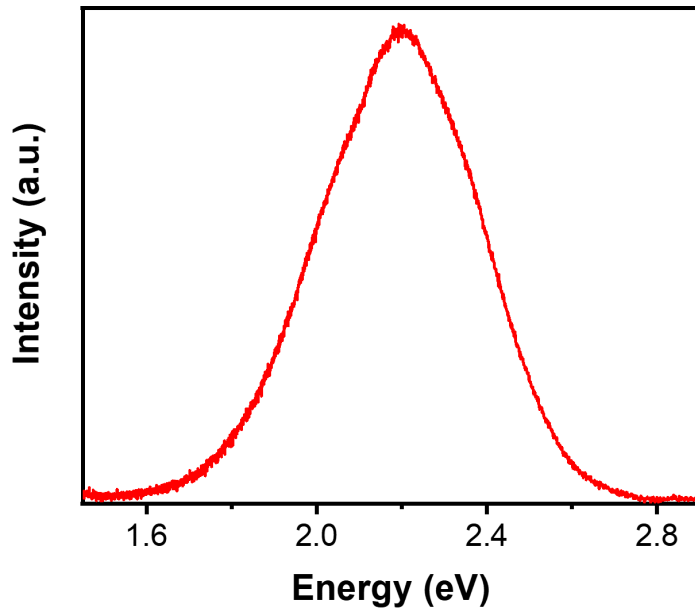


Fig. S5. Photoluminescence spectrum of commercial ZnO (Merck, CAS No:1314-13-2).

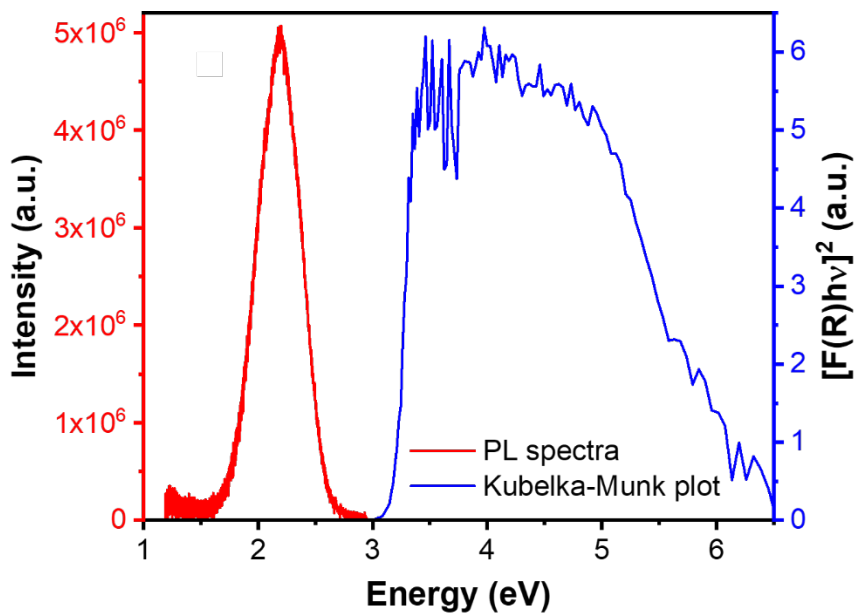


Fig. S6. Photoluminescence spectra and the Tauc plot of ZnO_U2 sample, revealing the presence of electronic state inside the bandgap caused by crystal defects.

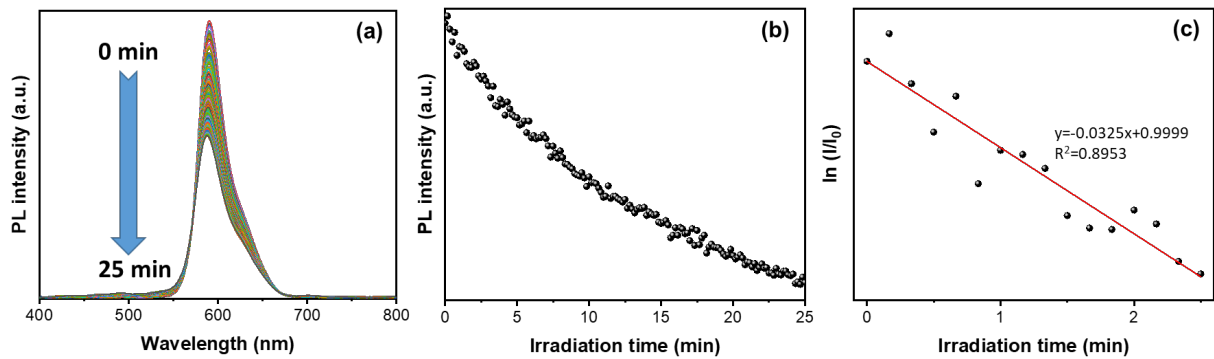


Fig. S7. Photodegradation of rhodamine B without the ZnO photocatalyst. (a) PL spectra with respect to irradiation time, (b) evolution of PL intensity, and (c) first-order kinetic plot.

References

- 1 R. Gao, Z. Liang, J. Tian, Q. Zhang, L. Wang and G. Cao, *Nano Energy*, 2013, **2**, 40–48.
- 2 R. Krishnapriya, S. Praneetha and A. Vadivel Murugan, *CrystEngComm*, 2015, **17**, 8353–8367.
- 3 M. Huang, S. Weng, B. Wang, J. Hu, X. Fu and P. Liu, *J. Phys. Chem. C*, 2014, **118**, 25434–25440.
- 4 R. Boppella, K. Anjaneyulu, P. Basak and S. V. Manorama, *J. Phys. Chem. C*, 2013, **117**, 4597–4605.
- 5 J. Chang, R. Ahmed, H. Wang, H. Liu, R. Li, P. Wang and E. R. Waclawik, *J. Phys. Chem. C*, 2013, **117**, 13836–13844.
- 6 S. Marković, I. Stojković Simatović, S. Ahmetović, L. Veselinović, S. Stojadinović, V. Rac, S. D. Škapin, D. Bajuk Bogdanović, I. Janković Častvan and D. Uskoković, *RSC Adv.*, 2019, **9**, 17165–17178.
- 7 T. R. Chetia, M. S. Ansari and M. Qureshi, *ACS Appl. Mater. Interfaces*, 2015, **7**, 13266–13279.
- 8 L. Wang, H. Li, S. Xu, Q. Yue and J. Liu, *Mater. Chem. Phys.*, 2014, **147**, 1134–1139.
- 9 E. A. Araújo Júnior, F. X. Nobre, G. da S. Sousa, L. S. Cavalcante, M. Rita de Moraes Chaves Santos, F. L. Souza and J. M. Elias de Matos, *RSC Adv.*, 2017, **7**, 24263–24281.
- 10 A. Iglesias-Juez, F. Viñes, O. Lamiel-García, M. Fernández-García and F. Illas, *J. Mater. Chem. A*, 2015, **3**, 8782–8792.
- 11 S. Marković, V. Rajić, A. Stanković, L. Veselinović, J. Belošević-Čavor, K. Batalović, N. Abazović, S. D. Škapin and D. Uskoković, *Solar Energy*, 2016, **127**, 124–135.
- 12 A. Stanković, Z. Stojanović, L. Veselinović, S. D. Škapin, I. Bračko, S. Marković and D. Uskoković, *Mater. Sci. Eng. B*, 2012, **177**, 1038–1045.
- 13 S. Kundu, S. Sain, T. Kar and S. K. Pradhan, *ChemistrySelect*, 2016, **1**, 3705–3712.
- 14 K. Davis, R. Yarbrough, M. Froeschle, J. White and H. Rathnayake, *RSC Adv.*, 2019, **9**, 14638–14648.
- 15 Y. V. Kaneti, Z. Zhang, J. Yue, Q. M. D. Zakaria, C. Chen, X. Jiang and A. Yu, *Phys. Chem. Chem. Phys.*, 2014, **16**, 11471–11480.
- 16 Y. V. Kaneti, J. Yue, X. Jiang and A. Yu, *J. Phys. Chem. C*, 2013, **117**, 13153–13162.

- 17 B. Liu, J. Xu, S. Ran, Z. Wang, D. Chen and G. Shen, *CrystEngComm*, 2012, **14**, 4582–4588.
- 18 B. Madavali, H.-S. Kim and S.-J. Hong, *Mater. Lett.*, 2014, **132**, 342–345.
- 19 Y. Liu, D. Huang, H. Liu, T. Li and J. Wang, *Cryst. Growth Des.*, 2019, **19**, 2758–2764.
- 20 V. Cauda, D. Pugliese, N. Garino, A. Sacco, S. Bianco, F. Bella, A. Lamberti and C. Gerbaldi, *Energy*, 2014, **65**, 639–646.